

ORIGINAL ARTICLE

Open Access

Synthesis, characterization and optical properties of zinc oxide nanoparticles

Surabhi Siva Kumar^{1*}, Putcha Venkateswarlu², Vanka Ranga Rao³ and Gollapalli Nageswara Rao⁴

Abstract

Zinc oxide nanoparticles were synthesized using a simple precipitation method with zinc sulfate and sodium hydroxide as starting materials. The synthesized sample was calcined at different temperatures for 2 h. The samples were characterized by X-ray diffraction (XRD), scanning electron microscopy (SEM), energy dispersive spectroscopy (EDS), and proton-induced X-ray emission (PIXE) analysis. SEM images show various morphological changes of ZnO obtained by the above method. The average crystallite sizes of the samples were calculated from the full width at half maximum of XRD peaks by using Debye-Scherrer's formula and were found to be in the nanorange. EDS shows that the above route produced highly pure ZnO nanostructures. PIXE technique was used for trace elemental analysis of ZnO. The optical band gaps of various ZnO powders were calculated from UV-visible diffuse reflectance spectroscopic studies.

Keywords: Nanostructures, Semiconductors, Chemical synthesis, Catalytic properties, Optical properties

Background

Nanosized particles of semiconductor materials have gained much more interest in recent years due to their desirable properties and applications in different areas such as catalysts [1], sensors [2], photoelectron devices [3,4], highly functional and effective devices [5]. These nanomaterials have novel electronic, structural, and thermal properties which are of high scientific interests in basic and applied fields. Zinc oxide (ZnO) is a wide band gap semiconductor with an energy gap of 3.37 eV at room temperature. It has been used considerably for its catalytic, electrical, optoelectronic, and photochemical properties [6-9]. ZnO nanostructures have a great advantage to apply to a catalytic reaction process due to their large surface area and high catalytic activity [10]. Since zinc oxide shows different physical and chemical properties depending upon the morphology of nanostructures, not only various synthesis methods but also the physical and chemical properties of synthesized zinc oxide are to be investigated in terms of its morphology.

Many methods have been described in the literature for the production of ZnO nanostructures such as laser

ablation [11], hydrothermal methods [12], electrochemical depositions [13], sol-gel method [14], chemical vapor deposition [15], thermal decomposition [16], and combustion method [17,18]. Recently, ZnO nanoparticles were prepared by ultrasound [19], microwave-assisted combustion method [20], two-step mechanochemical-thermal synthesis [21], anodization [22], co-precipitation [23], and electrophoretic deposition [24].

Rodrigues-Paez et al. synthesized zinc oxide nanoparticles with different morphologies by controlling different parameters of the precipitation process such as solution concentration, pH, and washing medium [25]. In the present study, ZnO nanostructures were synthesized using a simple precipitation method. Zinc sulfate heptahydrate and sodium hydroxide were used as precursors to formulate ZnO nanostructures. The prepared samples were characterized by X-ray diffraction (XRD) and scanning electron microscopy (SEM), and the purity of the sample was tested by energy dispersive spectroscopy (EDS) and proton-induced X-ray emission (PIXE) analysis. The band gap energies of the samples were calculated from diffuse reflectance spectroscopy. The morphology, crystallite size, and optical properties of ZnO nanostructures were investigated, and an attempt was made to correlate the optical properties of ZnO with morphology and crystallite size.

* Correspondence: siva_ks9123@rediffmail.com

¹Department of Chemistry, Anil Neerukonda Institute of Technology and Sciences, Sangivalasa, Visakhapatnam 531 162, India

Full list of author information is available at the end of the article

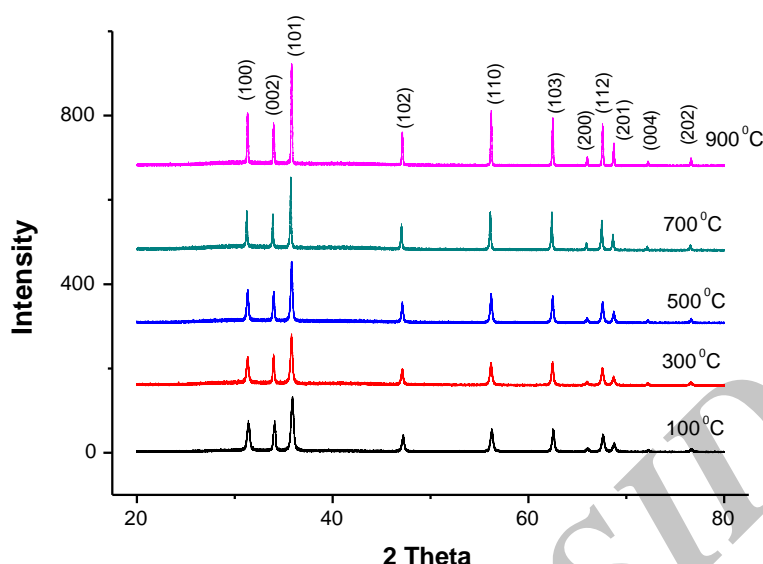


Figure 1 XRD patterns of ZnO-1 calcined at different temperatures.

Methods

Materials

Zinc sulfate heptahydrate and sodium hydroxide were used in the experiments. All the chemicals used were of analytical reagent grade obtained from Merck (Mumbai, India), and deionized water is used for the preparation of solutions.

Synthesis of ZnO

To the aqueous solution of zinc sulfate, sodium hydroxide solution was added slowly dropwise in a molar ratio of 1:2 under vigorous stirring, and the stirring was continued for 12 h. The precipitate obtained was filtered and washed thoroughly with deionized water. The precipitate was dried in an oven at 100°C and ground to fine powder using agate mortar [26]. The powder obtained from the above method was calcined at different temperatures such as 300°C, 500°C, 700°C, and 900°C for 2 h.

Characterization

XRD and SEM

The compounds were characterized for their structure and morphology by XRD and SEM. The XRD patterns of

the powdered samples were recorded using a Bruker D8 Advanced X-ray diffractometer (Bruker Optik GmbH, Ettlingen, Germany) with CuK α radiation ($\lambda = 1.5418 \text{ \AA}$, rated as 1.6 kW), and SEM images of the samples were taken using a Philips XL 30 ESEM scanning electron microscope (FEI-Philips Company, Hillsboro).

UV-vis diffuse reflectance spectroscopy

UV-vis spectroscopy was used to characterize the optical absorption properties of ZnO. The UV-vis absorption spectra of the samples were recorded in the wavelength range of 200 to 800 nm using a Shimadzu UV 3600 UV-vis-NIR spectrometer (Shimadzu Corporation, Kyoto, Japan) in diffuse reflectance mode using BaSO₄ as reference. Spectra were recorded at room temperature, and the data were transformed through the Kubelka-Munk function [27].

Proton-induced X-ray emission

Finely powdered samples were mixed with pure graphite in the ratio of 1:1 (150 mg each), homogenized, and pressed into a 13-mm-diameter pellet. PIXE measurements have been carried out on a 3-MV horizontal pelletron accelerator at the Institute of Physics, Bhubaneswar [28]. Proton beam was collimated to a diameter of 3 mm on the target. A Si(Li) detector was kept at 90° with respect to the beam direction. The detector has an active area of 30 mm² with a beryllium window having a thickness of 12 μm and an energy resolution of 170 eV at 5.9 keV. Integrated charge on the sample was measured using a current integrator, which was connected to the target holder. The X-rays coming out of the chamber

Table 1 Average crystallite size of ZnO obtained from XRD using Equation 1

Calcination temperature (°C)	Crystallite size, <i>D</i> (nm)
300	64
500	74
700	131
900	187

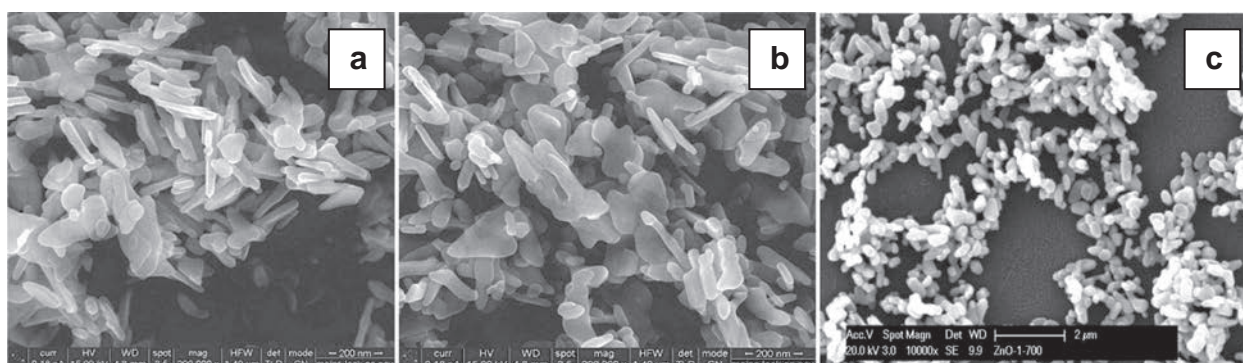


Figure 2 SEM images of ZnO samples calcined at three different temperatures. (a) 300°C, (b) 500°C, and (c) 700°C.

through a 95-μm Mylar window traveled through an air gap of 4 cm before entering the Si(Li) detector.

The targets were kept in the PIXE chamber at 45° to the beam. The Si(Li) detector is placed at 90° to the beam, and the beam current was kept in the range of 3 to 10 nA. Spectra were recorded using a Canberra MCA [29] (Canberra Industries, Meriden, CT, USA) and were transferred to a personal computer [30].

PIXE spectral analyses were carried out using GUPIX-95 [31] software that provides nonlinear least-square fitting of the spectrum. The thick-target PIXE analysis was performed since the target was thick enough to stop the proton beam entirely. To check the adopted analysis procedure and input parameters, external standard method was adopted using the macrometer standards and other certified reference materials, and accordingly, the values were normalized. Further details about the analysis procedure can be obtained from our earlier references [28,29].

Results and discussion

Catalyst characterization

XRD analysis

The XRD patterns of the ZnO powders prepared by the above method and calcined at different temperatures are

shown in Figure 1. All the diffraction peaks are well indexed to the hexagonal ZnO wurtzite structure (JCPDS no. 36-1451). Diffraction peaks corresponding to the impurity were not found in the XRD patterns, confirming the high purity of the synthesized products. The intensity of the peaks increases with calcination temperature, indicating increased crystallinity. A definite line broadening of diffraction peaks at 300°C, 500°C, and 700°C indicates that the synthesized materials are in the nanometer range. Table 1 shows the average crystallite sizes of the samples calculated by Debye-Scherrer's equation (Equation 1) using the full width at half maximum of 100, 002, and 101 of the X-ray diffraction peaks [32]. The average crystallite size increases with increase in calcination temperature. A significant increase in crystallite size is observed for the sample calcined at 900°C. At such high temperatures, migration of grain boundaries occurs, causing the coalescence of small grains and formation of large grains.

$$D = \frac{0.89\lambda}{\beta \cos\theta} \quad (1)$$

where D is the crystallite size (nm), λ is the wavelength

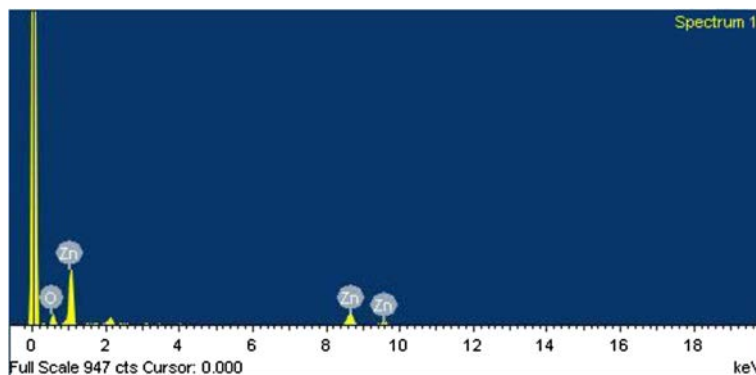


Figure 3 Energy dispersive spectra of ZnO calcined at 500°C.

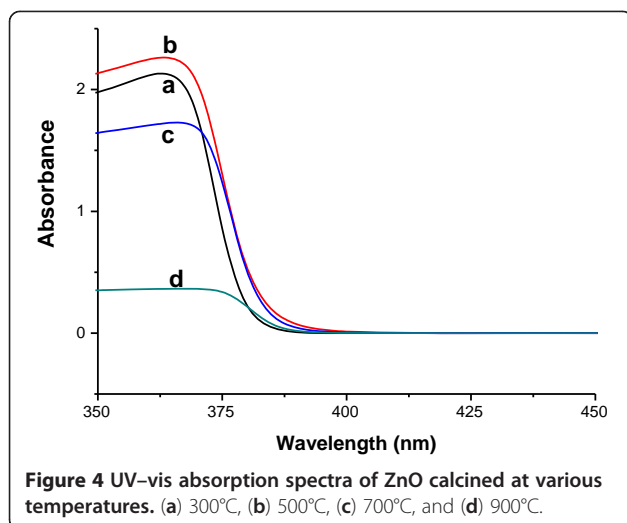


Figure 4 UV-vis absorption spectra of ZnO calcined at various temperatures. (a) 300°C, (b) 500°C, (c) 700°C, and (d) 900°C.

of incident X-ray (nm), β is the full width at half maximum, and θ is the diffraction angle.

SEM and EDS analysis

The SEM images of the samples are shown in Figure 2. The morphologies of ZnO are changed with calcination temperature. The samples calcined at 300°C and 500°C are nanoflakes which are turned to particles when calcined at 700°C. The SEM images of ZnO samples show that the agglomerations of particles are much less in this method of preparation. High-resolution SEM images of ZnO calcined at 300°C and 500°C (Figure 2b) show the presence of nanoparticles. The energy dispersive spectra of the samples obtained from the SEM-EDS analysis (Figure 3) clearly show that the sample prepared by the above route has pure ZnO phases.

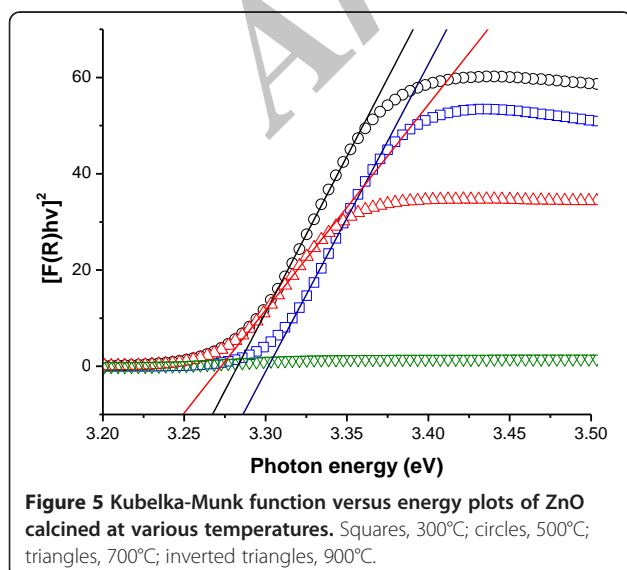


Figure 5 Kubelka-Munk function versus energy plots of ZnO calcined at various temperatures. Squares, 300°C; circles, 500°C; triangles, 700°C; inverted triangles, 900°C.

Table 2 Optical band gap of different ZnO samples calcined at different temperatures

Calcination temperature (°C)	Band gap (eV)
300	3.30
500	3.28
700	3.27

Diffuse reflectance analysis

The UV-visible absorption spectra of the samples are shown in Figure 4. All the samples have a strong absorption maximum below 400 nm. The absorption maximum of the samples calcined at 500°C and 700°C are shifted to higher wavelengths. This red shift can be attributed to the agglomerations in the samples [33]. The band gap energy of the samples are measured by the extrapolation of the linear portion of the graph between the modified Kubelka-Munk function $[F(R)/hv]^2$ versus photon energy ($h\nu$) [27], as shown in Figure 5. The samples calcined at 900°C have low reflectance, and it is difficult to calculate the band gap of these samples. The band gap of ZnO is decreased with an increase in calcination temperature. This is due to the increase in particle size of ZnO with calcination temperature. The band gaps of the samples are shown in Table 2.

PIXE analysis

The samples are analyzed using GUPIX software for the purity and trace elements present in the ZnO nanoparticles. The results shown in Table 3 indicate that the prepared ZnO nanoparticles are having 99.7% purity with contaminants like Fe and Ti at trace level. The PIXE spectrum of the ZnO nanoparticle calcined at 300°C (Figure 6) reflects the dominated characteristic peak of Zn. However, the pile-up continuum may contain the characteristic X-ray lines of the trace contaminants like Pb which cannot be observed in the spectra and could not be estimated due to increase in the minimum detection limit of the respective elements. The importance of effective suppression of the pile-up continuum is obvious in terms of the limit of detection of trace level contaminants. The pile-up continuum of major elements like Zn in this case may overlap the X-ray lines of trace elements; therefore, the limits of detection for those elements are worse. However, as the residual concentration is only within some thousands of

Table 3 Concentration of various elements in ZnO nanoparticles

Element	Concentration	Statistical error (%)
Ti	1,000 ppm	11
Fe	900 ppm	15
Zn	99.70%	0.1

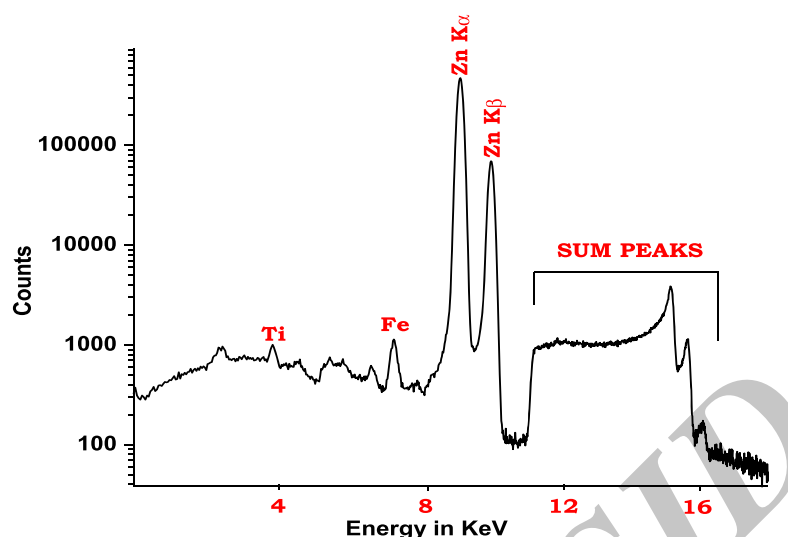


Figure 6 PIXE spectrum of ZnO calcined at 300°C.

parts per million, these individual elements must be much less in concentration if present and hence may not affect the purity of materials significantly. So, the PIXE study confirms the effectiveness of our nanoparticle preparation procedure.

Conclusions

ZnO nanoparticles were prepared using a simple precipitation method. The XRD and EDS analyses clearly indicate that highly pure ZnO is formed in the above method. SEM images of ZnO show that the morphology was changed with calcination temperature. PIXE analysis confirmed that the prepared material has a high purity and the presence of elements like Fe and Ti in trace level. The band gap of ZnO was decreased by an increase in calcination temperature, and the absorption maximum is also shifted to higher wavelengths.

Competing interests

The authors declare that they have no competing interests.

Authors' contributions

SS was involved in the acquisition, analysis, and interpretation of data. PV was involved in getting the PIXE data and analysis. VR was involved in designing the experimental work and drafting the manuscript. GN revised the manuscript critically and gave final approval for submission. All authors read and approved the final manuscript.

Acknowledgment

SSK is indebted to the UGC Networking program, University of Hyderabad for providing instrumental facility to carry out the XRD and SEM analyses. The authors are thankful to the Institute of Physics for giving permission to carry out the PIXE analysis.

Author details

¹Department of Chemistry, Anil Neerukonda Institute of Technology and Sciences, Sangivalasa, Visakhapatnam 531 162, India. ²Department of Physics, Anil Neerukonda Institute of Technology and Sciences, Sangivalasa, Visakhapatnam 531 162, India. ³Department of Chemistry, Government

College (Autonomous), Rajahmundry 533 105, India. ⁴School of Chemistry, Andhra University, Visakhapatnam 530 003, India.

Received: 9 September 2012 Accepted: 28 April 2013
Published: 7 May 2013

References

- Joshi, SS, Patil, PR, Naimase, MS, Bakare, PP: Role of ligands in the formation, phase stabilization, structural and magnetic properties of α -Fe₂O₃ nanoparticles. *J. Nanopart. Res.* **5**, 635–643 (2006)
- Cheng, XL, Zhao, H, Huo, LH, Gao, S, Zhao, JG: ZnO nanoparticulate thin film: preparation, characterization and gas-sensing properties. *Sens. Actuators B.* **102**, 248–252 (2004)
- Lee, SY, Shim, ES, Kang, HS, Pang, SS: Fabrication of ZnO thin film diode using laser annealing. *Thin Solid Films.* **437**, 31–34 (2005)
- Wang, ZL, Kong, XY, Ding, Y, Gao, P, Hughes, WL: Semiconducting and piezoelectric oxide nanostructures induced by polar surfaces. *Adv. Funct. Mater.* **14**, 943–956 (2004)
- Huang, YH, Zang, Y, Liu, L, Fan, SS, Wei, Y, He, J: Controlled synthesis and field emission properties of ZnO nanostructures with different morphologies. *J. Nanosci. Nanotechnol.* **6**, 787–790 (2006)
- Brida, D, Fortunato, E, Ferreira, I, Aguas, H, Martins, R: New insights on large area flexible position sensitive detectors. *J. Non-Cryst. Solids.* **299**, 1272–1276 (2002)
- Wang, ZL: Zinc oxide nanostructures: growth properties and applications. *J. Phys. Condens. Matter.* **16**, R829–R858 (2004)
- Suchea, M, Christoulakis, S, Moschovis, K, Katsarakis, N, Kiriakidis, G: ZnO transparent thin films for gas sensor applications. *Thin Solid Films.* **515**, 551–554 (2006)
- Ashour, A, Kaid, MA, El-Syed, NZ, Ibrahim, AA: Physical properties of ZnO thin films deposited by spray pyrolysis technique. *Appl. Surf. Sci.* **252**, 7844–7848 (2006)
- Chen, JC, Tang, CT: Preparation and application of granular ZnO/Al₂O₃ catalyst for the removal of hazardous trichloroethylene. *J. Hazard. Mater.* **142**, 88–96 (2007)
- Scarisoareanu, N, Metai, DG, Dinescu, G, Epurescu, G, Ghica, C, Nistor, LC, Dinescu, M: Properties of ZnO thin films prepared by radio-frequency plasma beam assisted laser ablation. *Appl. Surf. Sci.* **247**, 518–525 (2005)
- Ni, YH, Wei, XW, Hong, JM, Ye, Y: Hydrothermal synthesis and optical properties of ZnO nanorods. *Mater. Sci. Eng., B, Solid State Mater. Adv. Technol.* **121**, 42–47 (2005)
- Chang, S, Yoon, SO, Park, HJ, Sakai, A: Luminescence properties of Zn nanowires prepared by electrochemical etching. *Mater. Lett.* **53**, 432–436 (2002)
- Ristić, M, Musić, S, Ivanda, M, Popović, S: Sol–gel synthesis and characterization of nanocrystalline ZnO powders. *J. Alloys Compd.* **397**, L1–L4 (2005)

15. Wu, JJ, Liu, SC: Low-temperature growth of well-aligned ZnO nanorods by chemical vapor deposition. *Adv. Mater.* **14**, 215–218 (2002)
16. Wang, RC, Tsai, CC: Efficient synthesis of ZnO nanoparticles, nanowalls, and nanowires by thermal decomposition of zinc acetate at a low temperature. *Appl. Phys. A*. **94**, 241–245 (2009)
17. Lamas, DG, Lascalea, GE, Walsoc, NE: Synthesis and characterization of nanocrystalline powders for partially stabilized zirconia ceramics. *J. Eur. Ceram. Soc.* **18**, 1217–1221 (1998)
18. Badhuri, S, Badhuri, SB: Enhanced low temperature toughness of $\text{Al}_2\text{O}_3\text{-ZrO}_2$ nano/nano composites. *Nanostruct. Mater.* **8**, 755–763 (1997)
19. Khorsand, Z, Abid, A, Majid, WH, Wang, HZ, Yousefi, R, Golsheikh, M, Ren, ZF: Sonochemical synthesis of hierarchical ZnO nanostructures. *Ultrasonic Sonochemistry* **20**, 395–400 (2013)
20. Kooti, M, Nagdhi Sedish, A: Microwave-assisted combustion synthesis of ZnO nanoparticles. *J. Chem.* (2013). doi:10.1155/2013/562028
21. Rajesh, D, Vara Lakshmi, B, Sunandana, CS: Two-step synthesis and characterization of ZnO nanoparticles. *Physica B-Cond. Mater.* **407**, 4537–4539 (2012)
22. Shetty, A, Nanda, K: Synthesis of zinc oxide porous structures by anodisation with water as an electrolyte. *Appl. Phys. A*. **109**, 151–157 (2012)
23. Singh, O, Kohli, N, Singh, RC: Precursor controlled morphology of zinc oxide and its sensing behavior. *Sens. Actuators B*. **178**, 149–154 (2013)
24. Vazquez, A, Lopez, IA, Gomez, I: Growth mechanism of one-dimensional zinc sulfide nanostructures through electrophoretic deposition. *J. Mater. Sci* **48**, 2701–2704 (2013)
25. Rodrigues-Paez, J, Caballero, AC, Villegas, M, Moure, C, Duran, P, Fernandez, JF: Controlled precipitation methods: formation mechanism of ZnO nanoparticles. *J. Eur. Ceram. Soc.* **21**, 925–930 (2001)
26. Daneshvar, N, Aber, S, Sayed Dorraji, MS, Khataee, AR, Rasoulifard, MH: Preparation and investigation of photocatalytic properties of ZnO nanocrystals: effect of operational parameters and kinetic study. *Int. J. Chem. Biom. Eng* **1**(1), 24–29 (2008)
27. Cimitan, S, Albonetti, S, Forni, L, Peri, F, Lazzari, D: Solvothermal synthesis and properties control of doped ZnO nanoparticles. *J. Colloid. Interface Sci.* **329**, 73–80 (2009)
28. Vijayan, V, Ramamurthy, VS, Behera, SN, Puri, S, Shanti, JS, Singh, N: Elemental composition of fly ash from a coal fired thermal power plant: a study using PIXE and EDXRF. X-ray spectrometry. **26**, 65–68 (1997)
29. Vijayan, V, Nayak, PK, Chakrovorty, V: Proton induced X-ray emission studies on Indian copper coins. *Ind. J. Phys. A*. **76**, 477–479 (2002)
30. Maxwell, JA, Teesdale, WJ, Campbell, JL: The Guelph PIXE software package II. *Nucl. Instrum. Methods B*. **95**, 407–421 (1995)
31. Gleiter, H: Nanocrystalline materials. *Prog. Mater. Sci.* **33**, 223–315 (1989)
32. Chen, CC, Liu, P, Lu, CH: Synthesis and characterization of nano-sized ZnO powders by direct precipitation method. *Chem. Eng. J.* **144**, 509–513 (2008)
33. Babita, B, Kishore Kumar, D, Manorama, SV: Hydrothermal synthesis of highly crystalline ZnO nanoparticles: a competitive sensor for LPG and EtOH. *Sens. Actuators B*. **119**, 676–682 (2006)

doi:10.1186/2228-5326-3-30

Cite this article as: Kumar et al.: Synthesis, characterization and optical properties of zinc oxide nanoparticles. *International Nano Letters* 2013 3:30.

Submit your manuscript to a SpringerOpen[®] journal and benefit from:

- Convenient online submission
- Rigorous peer review
- Immediate publication on acceptance
- Open access: articles freely available online
- High visibility within the field
- Retaining the copyright to your article

Submit your next manuscript at ► springeropen.com